


RESEARCH PAPER



The role of mitochondria in anchoring dynein to the cell cortex extends beyond clustering the anchor protein

Heidi L. Schmit*, Lauren M. Kraft*, Conor F. Lee-Smith*, and Laura L. Lackner 

Department of Molecular Biosciences, Northwestern University, Evanston, IL, USA

ABSTRACT

Organelle distribution is regulated over the course of the cell cycle to ensure that each of the cells produced at the completion of division inherits a full complement of organelles. In yeast, the protein Num1 functions in the positioning and inheritance of two essential organelles, mitochondria and the nucleus. Specifically, Num1 anchors mitochondria as well as dynein to the cell cortex, and this anchoring activity is required for proper mitochondrial distribution and dynein-mediated nuclear inheritance. The assembly of Num1 into clusters at the plasma membrane is critical for both of its anchoring functions. We have previously shown that mitochondria drive the assembly of Num1 clusters and that these mitochondria-assembled Num1 clusters serve as cortical attachment sites for dynein. Here we further examine the role for mitochondria in dynein anchoring. Using a GFP- α GFP nanobody targeting system, we synthetically clustered Num1 on eisosomes to bypass the requirement for mitochondria in Num1 cluster formation. Utilizing this system, we found that mitochondria positively impact the ability of synthetically clustered Num1 to anchor dynein and support dynein function even when mitochondria are no longer required for cluster formation. Thus, the role of mitochondria in regulating dynein function extends beyond simply concentrating Num1; mitochondria likely promote an arrangement of Num1 within a cluster that is competent for dynein anchoring. This functional dependency between mitochondrial and nuclear positioning pathways likely serves as a mechanism to order and integrate major cellular organization systems over the course of the cell cycle.

ARTICLE HISTORY

Received 29 March 2018
Accepted 16 May 2018

KEYWORDS

Mitochondrial positioning;
dynein; inter-organelle
contact sites

Introduction

Eukaryotic cells have membrane-bound organelles, which create unique environments for a variety of critical cellular functions. Many essential organelles, such as mitochondria and the nucleus, cannot be generated *de novo* and need to be faithfully inherited to maintain cell viability. In dividing cells, the inheritance of many organelles requires active positioning mechanisms that function to transport and retain organelles at specific cellular locations. The positioning mechanisms for distinct organelles must be coordinated with each other as well as with the cell cycle to ensure that each daughter cell receives the appropriate complement of organelles.


In the asymmetrically dividing budding yeast *Saccharomyces cerevisiae*, the plasma membrane-associated protein Num1 functions in the inheritance and positioning of both mitochondria and the nucleus. Num1, originally identified as a player in nuclear

migration, serves to anchor dynein to the cell cortex, where dynein captures and walks along astral microtubules to help orient the mitotic spindle [1–7]. More recently, a role for Num1 in mitochondrial distribution and inheritance has been described [8–10]. Specifically, Num1 is the core component of the mitochondria-ER-cortex anchor (MECA), which functions to tether mitochondria to the plasma membrane and impacts the distribution and inheritance of the organelle [10]. Thus, the anchoring activity of Num1 is required for proper dynein-mediated nuclear inheritance as well as mitochondrial distribution.

Num1 is a 313 kD protein that contains an N-terminal coiled-coil (CC) domain, an EF hand-like motif, a region of twelve 64 amino acid repeats, and a C-terminal pleckstrin homology (PH) domain [1]. The CC and PH domains are critical for both of Num1's anchoring functions. The CC domain interacts directly with the mitochondrial membrane and

CONTACT Laura L. Lackner  Laura.Lackner@northwestern.edu

*These authors contributed equally to this work.

 Supplemental data for this article can be accessed [here](#).

is also required for the Num1-dynein interaction [10–12]. The PH domain, which binds with high specificity to $PI_{4,5}P_2$, targets Num1 to the plasma membrane [13,14], where the protein is found in clusters as well as in a pool that is diffusely localized along the plasma membrane and with cortical ER [3,5,10,15,16]. Cluster formation, which is dependent on the CC domain and an interaction with mitochondria (Figure 1(a)), is critical for the function of Num1 in both mitochondria and dynein anchoring [10,11,17]. Cluster formation has been proposed to enhance the interaction between Num1 and its membrane and protein binding partners and, consequently, the ability of Num1 to robustly tether mitochondria and dynein to the cell cortex [10,11]. In addition, Num1 is proposed to directly activate dynein [18,19]. Thus, increasing the effective concentration of Num1 via cluster formation may also enhance dynein activation at sites of anchoring.

While dynein is not required for Num1-mediated mitochondrial anchoring [10,11], mitochondria drive the assembly of Num1 clusters that serve as cortical attachment sites for dynein [17]. These results raise the question of whether the role for mitochondria in dynein anchoring is to simply concentrate Num1 or whether mitochondria play an additional role in driving the assembly of a structure competent to tether dynein. To address this question, we used a GFP- α GFP nanobody targeting system to synthetically cluster Num1 on eisosomes, a discrete plasma membrane compartment [20], and bypassed the requirement for mitochondria to drive Num1 cluster formation. Using this system, we found that the presence of mitochondria at synthetically clustered Num1 positively correlated with the ability of a cluster to anchor dynein. Thus, the influence of mitochondria on dynein function extends beyond simply concentrating Num1.

Results

Num1 can be synthetically clustered at the cell cortex

Our approach for synthetically clustering Num1 on the plasma membrane was to target the protein

to eisosomes. Eisosomes are discrete plasma membrane compartments composed of more than 15 proteins that assemble into stable, stationary, plasma membrane-associated complexes [20,21]. Around 20–50 eisosomes are present per cell, and the two core components, Pil1 and Lsp1, are present in 2,000–5,000 copies per eisosome [20]. We reasoned that by targeting Num1 to eisosomes we would be able to concentrate Num1 in discrete clusters at the cell cortex independent of an interaction with mitochondria. To target Num1 to eisosomes, we used a GFP- α GFP nanobody targeting system (Figure 1(a)). The α GFP nanobody is a ~ 16 kD, monomeric, single domain antibody that binds GFP with high affinity [22,23]. We engineered cells to express Pil1 as an α GFP nanobody fusion (Pil1- α GFP) from the endogenous *PIL1* locus. We then expressed a yEGFP fusion of Num1 that lacks the PH domain (Num1 Δ PH) from the endogenous *NUM1* locus (Figure 1(a and b)). The PH domain is required to target the protein to the plasma membrane, and, as expected, Num1 Δ PH exhibited a primarily diffuse cytosolic localization with occasional non-cortical clusters observed (Figure 1(c)) [10,14]. In contrast, in the presence of Pil1- α GFP, Num1 Δ PH localized to discrete clusters at the cell cortex, indicating the protein was effectively targeted to eisosomes (Figure 1(c)). The eisosome-associated clusters of Num1 Δ PH will be referred to as Pil1-associated Num1 or PAN clusters (Figure 1(a)), and cells expressing Pil1- α GFP and Num1 Δ PH will be referred to as PAN cells. In agreement with targeting to eisosomes, PAN clusters robustly colocalized with Lsp1 while wildtype Num1 clusters did not (Figure 1(d)). PAN clusters were more abundant than clusters formed by wildtype Num1 (Figure 1(c)), which is consistent with the idea that targeting Num1 Δ PH to eisosomes drives cluster formation in a manner distinct from wildtype Num1. Consistently, in contrast to wildtype Num1 cluster formation which depends on the CC domain of the protein [10,11], PAN clusters were no longer dependent on the CC domain as PAN Δ CC formed clusters indistinguishable from PAN (Figure 1(c)). Together, these results indicate that Pil1- α GFP is able to target and synthetically cluster Num1 Δ PH on the plasma membrane.

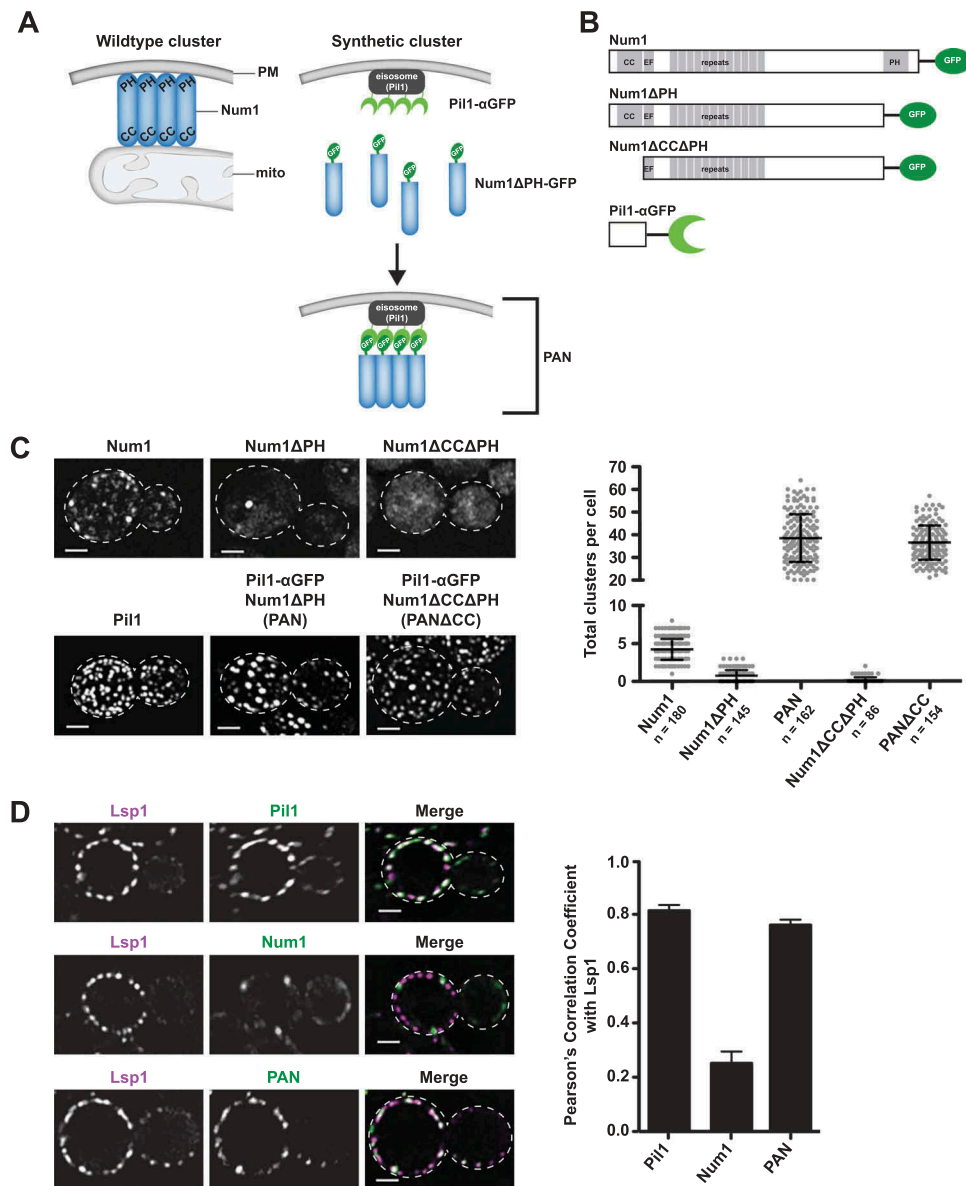


Figure 1. A system to synthetically cluster Num1 at the cell cortex. (A and B) The GFP- α GFP nanobody targeting system used to synthetically cluster Num1 on the plasma membrane. The schematic on the left in A depicts a wildtype Num1 cluster, which assembles only in the presence of mitochondria. The schematic on the right in A depicts mitochondria-independent assembly of a synthetic Num1 cluster driven by the GFP- α GFP nanobody targeting system. Schematics of constructs used in the study are shown in B. CC, coiled-coil domain; EF, EF hand-like domain; mito, mitochondria; PAN, Pil1-associated Num1; PH, pleckstrin homology domain; PM, plasma membrane; α GFP, α GFP nanobody. (C) Cells expressing Pil1, Num1, Num1 Δ PH, PAN, Num1 Δ CC Δ PH, or PAN Δ CC as GFP fusions were analyzed by fluorescence microscopy. Deconvolved, maximum intensity, whole cell Z-projections are shown. The cell cortex is outlined with a dashed white line. Bar, 2 μ m. Quantification of the total number of clusters per cell is shown as the mean \pm SD indicated. n = the number of cells quantified, as indicated in the figure. (D) Cells expressing Lsp1-mKate and Pil1, Num1, or PAN as GFP fusions were analyzed by fluorescence microscopy. Single focal planes of deconvolved Z-stacks are shown. The cell cortex is outlined with a dashed white line. Bar, 2 μ m. The Pearson's correlation between Lsp1 and the indicated GFP fusion is shown as the mean \pm SD of 10 fields of view with at least 15 cells per field.

Synthetically clustered Num1 tethers mitochondria

We next examined the relationship between PAN clusters and mitochondria. We found that

mitochondria were persistently localized to a subset of PAN clusters, indicating that PAN is able to interact with and tether mitochondria to the cell cortex (Figure 2(a and b)). The persistent

localization of mitochondria with PAN clusters significantly decreased in the absence of the CC domain of Num1 (Figure 2(a and b)). Thus, the interaction between PAN clusters and mitochondria is dependent on the known mitochondria interaction domain [10–12]. The number of mitochondria-associated wildtype Num1 clusters per cell ranged from 1–7 with an average of 4, while the mitochondria-

associated PAN clusters per cell ranged from 3–19 with an average of 8 (Figure 2(b)). The increased number of mitochondria-associated clusters in PAN cells may be a result of two non-mutually exclusive possibilities: 1) there is an increase in the level of Num1 protein in PAN cells compared to wildtype cells (Fig. S1), or 2) clustering of Num1 is a limiting step in the formation of a mitochondria tether point.

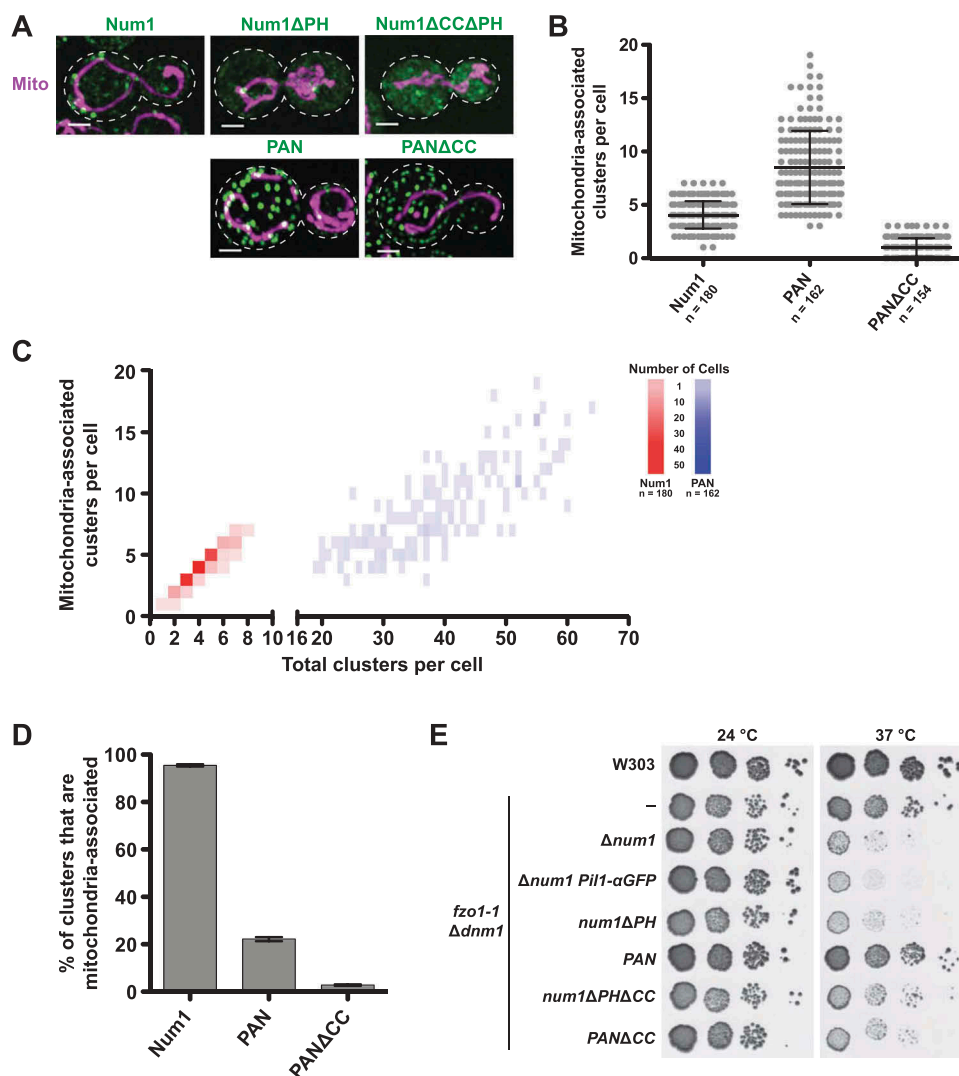


Figure 2. The relationship between PAN clusters and mitochondria. (A) Cells expressing Num1, Num1 Δ PH, PAN, Num1 Δ CC Δ PH, or PAN Δ CC as GFP fusions along with mitoRED were analyzed by fluorescence microscopy. Deconvolved, maximum intensity, whole cell Z-projections are shown. The cell cortex is outlined with a dashed white line. Bar, 2 μ m. (B) Quantification of the number of mitochondria-associated clusters per cell in cells expressing Num1, PAN, and PAN Δ CC along with mitoRED. To be considered a mitochondria-associated cluster, mitochondria had to remain associated with a cluster for ≥ 1.5 min. Each dot represents a cell. The mean \pm SD are shown. n = the number of cells quantified, as indicated in the figure. (C) A plot of the number of mitochondria-associated Num1 and PAN clusters per cell versus the total number of clusters per cell. The color of each rectangle represents the number of cells, as indicated by the key, with that number of total and mitochondria-associated clusters. n = the number of cells quantified, as indicated in the figure. (D) Mitochondria-associated Num1, PAN, and PAN Δ CC clusters per cell as a percentage of total clusters per cell. n = 3 independent experiments in which ≥ 50 cells were counted. The mean \pm SD is shown. (E) To assess growth, serial dilutions of the indicated strains were plated on rich medium and grown at the permissive (24°C) or non-permissive (37°C) temperature for the temperature sensitive *fzo1-1* allele, as indicated.

In the vast majority of cells expressing wildtype Num1, the number of mitochondria-associated clusters was equivalent to the total number of clusters per cell (Figure 2(c)), consistent with mitochondria-dependent cluster assembly [17]. In contrast, in all cells expressing PAN, the number of mitochondria-associated clusters was far lower than the total number of clusters per cell (Figure 2(c)). On average, ~95% of wildtype Num1 clusters were mitochondria-associated, while only ~21% of PAN clusters were associated with mitochondria (Figure 2(d)). The percentage of clusters that were mitochondria-associated further decreased in cells expressing PAN Δ CC, as was expected for the loss of the mitochondria interaction domain. Together these results indicate that, although PAN clusters can interact with and tether mitochondria, PAN cluster formation is independent of an interaction with mitochondria.

The mitochondrial tethering activity of Num1 is essential in the absence of the mitochondrial division and fusion proteins, Dnm1 and Fzo1, respectively [10]. We have previously shown that synthetic constructs that tether mitochondria to the plasma membrane can rescue the severe growth defect of *fzo1-1* Δ *dnm1* Δ *num1* cells grown at the non-permissive temperature for the *fzo1-1* temperature sensitive allele [10,24]. To further examine the mitochondrial tethering activity of PAN, we tested the ability of PAN to rescue the conditional growth defect of *fzo1-1* Δ *dnm1* Δ *num1* cells (Figure 2(e)). At the non-permissive temperature, *fzo1-1* Δ *dnm1* *num1* Δ *PH* cells as well as *fzo1-1* Δ *dnm1* Δ *num1* cells expressing only Pil1- α GFP exhibited a severe growth defect. In contrast, the expression of PAN rescued the growth of the conditional triple mutant, and the rescue by PAN was dependent on the presence of the CC domain. These results are consistent with the ability of PAN clusters to tether mitochondria. Therefore, using the GFP- α GFP nanobody targeting system, we are able to synthetically cluster Num1 in a manner in which the protein retains its ability to tether mitochondria but is no longer dependent on mitochondria to concentrate in clusters at the cell cortex.

Synthetic Num1 clusters function in dynein-mediated nuclear inheritance

We next examined if PAN clusters were able to anchor dynein to the cell cortex, which is required

for dynein-mediated nuclear inheritance [5]. Yeast have two partially redundant nuclear positioning pathways: the dynein- and Kar9-mediated pathways [2,25,26]. In the absence of both pathways, cells exhibit a severe growth defect or are inviable. To examine the function of PAN clusters in the dynein-mediated pathway, we tested the ability of PAN to rescue the lethality of Δ *kar9* Δ *num1* cells (Figure 3(a)). In contrast to the severe growth defect observed for Δ *kar9* *num1* Δ *PH* cells, Δ *kar9* PAN cells grew similarly to Δ *kar9* cells. These results indicate that PAN clusters are able to function in dynein-mediated nuclear inheritance.

We also examined spindle orientation as a readout for dynein function in PAN cells (Figure 3(b)) [2]. Cells expressing Num1 Δ PH exhibited an increase in spindle misorientation similar to Δ *dyn1* and Δ *num1* cells (Figure 3(c)). In contrast, the percentage of PAN cells with misoriented spindles was similar to wildtype cells, indicating PAN clusters can support dynein function (Figure 3(c)). Furthermore, in a Δ *kar9* background, PAN was still able to rescue spindle orientation (Figure 3(d)). Compared to Δ *kar9* *num1* Δ *PH* cells, in which misoriented spindles were observed in ~74% of cells, the percentage of cells with misoriented spindles in Δ *kar9* PAN cells was similar to Δ *kar9* cells, ~45%. Thus, the function of PAN in spindle positioning is specific to the dynein-mediated pathway.

Dynein associates with mitochondria-associated synthetic Num1 clusters

Our data indicate that PAN clusters can support dynein activity and, therefore, should be functional as dynein anchors. In contrast to wildtype Num1, in which the vast majority of clusters are mitochondria-associated, only a subset of PAN clusters are associated with mitochondria (Figure 2(c and d)) [17]. To determine if dynein is indeed anchored by PAN clusters and, if so, whether it exhibits a preference for mitochondria-associated PAN clusters, we simultaneously imaged PAN, Dyn1, and mitochondria. We observed that cortical dynein foci persistently colocalized with PAN clusters (Figure 4(a)), consistent with the ability of PAN clusters to anchor dynein. Importantly, we found that mitochondria

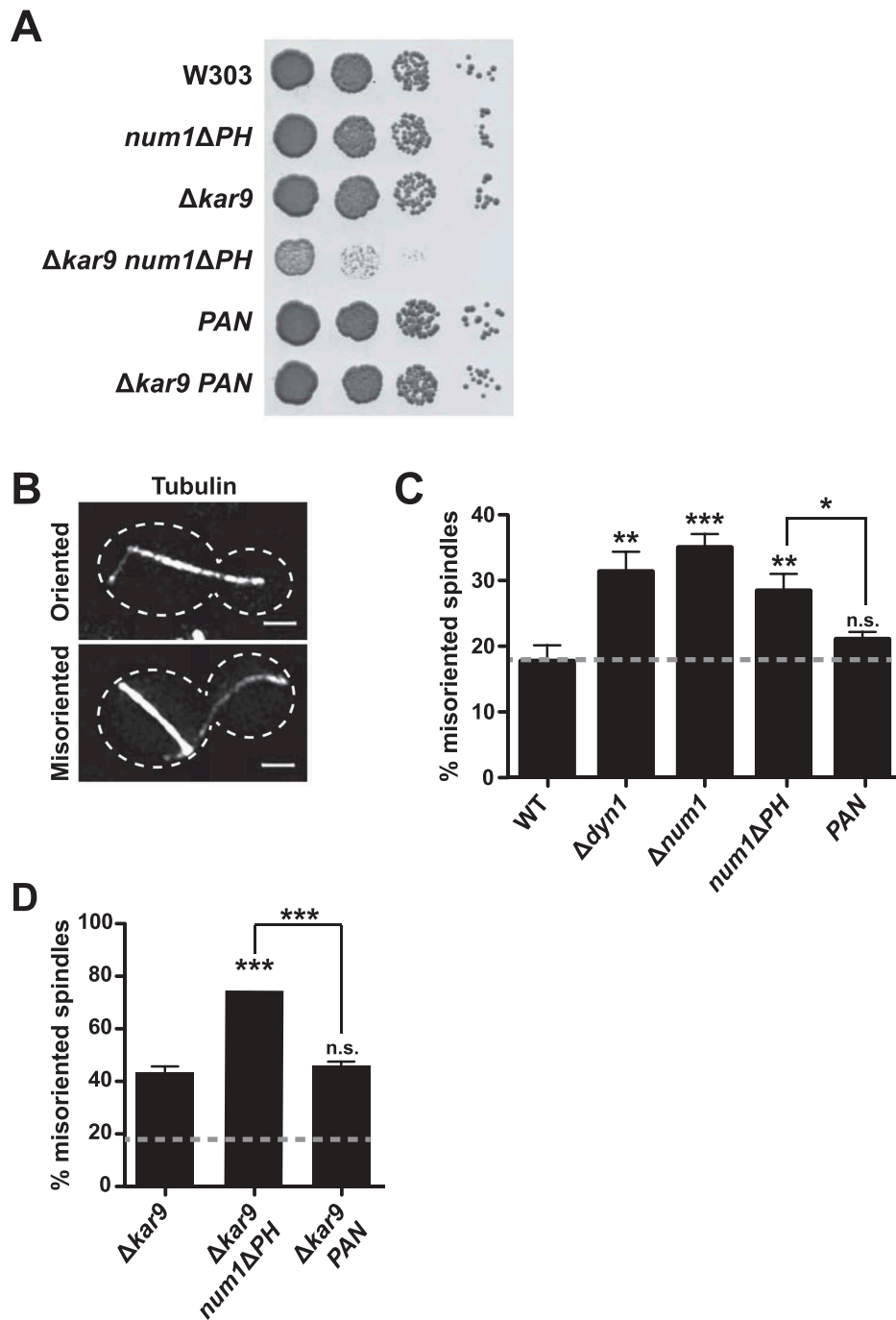


Figure 3. PAN clusters support dynein function. (A) To assess growth, serial dilutions of the indicated strains were plated on rich medium and grown at 30°C. (B–C) Wildtype W303, $\Delta dyn1$, $\Delta num1$, $num1\Delta PH$, and PAN cells expressing Ruby-Tub1 were visualized by fluorescence microscopy. Representative, deconvolved, maximum intensity, whole cell Z-projections of cells with spindles scored as correctly oriented and misoriented are shown (B). The cell cortex is outlined with a dashed line. Bars, 2 μm . Quantification of the percent of cells with misoriented spindles is shown as the mean \pm SD (C). Large buds with spindles > 1.25 μm were scored. $n = 3$ independent experiments of ≥ 52 spindles for each experiment. The dashed line represents the mean wildtype spindle misorientation value. p values are in comparison to wildtype W303 unless otherwise denoted by brackets. *** $p < 0.001$, ** $p < 0.01$, * $p < 0.02$; n.s., not significant. (D) Misoriented spindles in $\Delta kar9$, $\Delta kar9 num1\Delta PH$, and $\Delta kar9 PAN$ were quantified as described in C. The dashed line represents the mean wildtype spindle misorientation value from panel C. p values are in comparison to $\Delta kar9$ unless otherwise denoted by brackets. *** $p < 0.001$; n.s., not significant.

were also present at the vast majority of sites where cortical dynein foci and PAN clusters colocalized (Figure 4(a and b)). The percent of

cortical dynein foci that colocalized with both PAN clusters and mitochondria (~ 84%) was strikingly similar to the percent of cortical dynein

foci that colocalized with both wildtype Num1 clusters and mitochondria (~ 86%; Figure 4(a and b)) [17]. This was particularly notable given the fact that only ~ 21% of PAN clusters are

mitochondria-associated, while ~ 95% of wildtype Num1 clusters are mitochondria-associated (Figure 2(d)). Thus, the number of cortical dynein foci that colocalized with mitochondria-

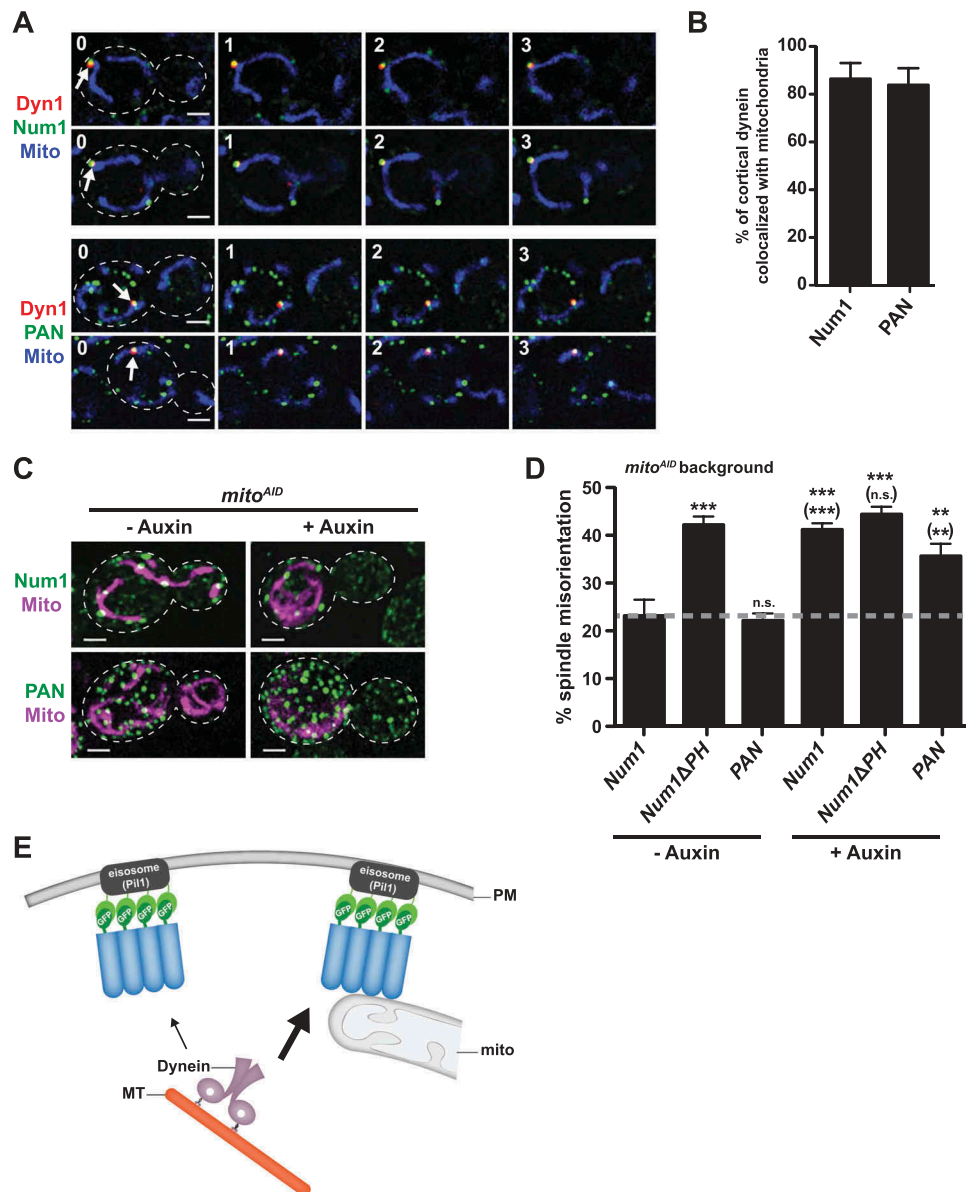


Figure 4. Mitochondria-associated PAN clusters anchor dynein. (A) *NUM1-yEGFP* or *PAN* cells expressing *Dyn1-mKate* and *mitoBFP* were visualized by fluorescence microscopy over time. Single focal planes of deconvolved Z-stacks are shown. Arrows indicate a colocalization event. The cell cortex is outlined with a dashed line. Bars, 2 μ m. Time is in minutes. (B) Quantification of the percent of cortical dynein foci that colocalize with mitochondria. $n \geq 103$ cortical dynein foci. Standard error of proportion is shown. To be considered cortically anchored, a *Dyn1-mKate* focus had to remain stable at the cell cortex for ≥ 1.5 minutes. (C) *mito^{AID} NUM1-yEGFP* and *mito^{AID} PAN* cells expressing *mitoRED* were grown in the absence or presence of auxin and visualized by fluorescence microscopy. Deconvolved, maximum intensity, whole cell Z-projections are shown. The cell cortex is outlined with a dashed white line. Bar, 2 μ m. (D) *mito^{AID} NUM1-yEGFP*, *mito^{AID} num1 Δ PH*, and *mito^{AID} PAN* cells expressing *Ruby-Tub1* and *mitoBFP* were visualized by fluorescence microscopy. Misoriented spindles were quantified as described in Figure 3(c). $n = 3$ independent experiments of ≥ 46 spindles for each experiment. The mean \pm SD is shown. p values are in comparison to wildtype *NUM1* cells, and p values in parentheses are in comparison to the identical genotype in the absence of auxin. *** $p < 0.001$, ** $p < 0.01$; n.s., not significant. (E) Model: The anchoring of dynein at the cell cortex by Num1 clusters assembled in the absence of mitochondria using the GFP- α GFP nanobody targeting system is positively influenced by the presence of mitochondria at a cluster.

associated PAN clusters was 4 times greater than what would be expected if mitochondria had no influence on the ability of PAN clusters to anchor dynein. These data indicate that mitochondria impact the ability of Num1 to anchor dynein even when the requirement for mitochondria in cluster formation has been bypassed.

Previously, we have shown that in the absence of mitochondrial inheritance, Num1 clusters do not form in buds and dynein function in spindle orientation is disrupted [17]. As the formation of PAN clusters does not depend on mitochondria, PAN clusters should still be present in buds that do not inherit mitochondria. To test this directly, we used a conditional mitochondrial inheritance strain, *mito^{AID}* [17]. This strain lacks Ypt11, one of the two adaptors required for Myo2-driven transport of mitochondria to the bud, and expresses the other adaptor, Mmr1, as a fusion to an auxin-inducible degron (AID). Consequently, the inheritance of mitochondria by buds in *mito^{AID}* cells is inhibited in the presence of auxin (Figure 4(c)) [17]. We observed PAN clusters in buds that inherited mitochondria as well as in those that lacked mitochondria (Figure 4(c)), consistent with mitochondria-independent cluster formation. We next examined spindle orientation in *mito^{AID}* PAN cells in the absence and presence of auxin. Similar to *mito^{AID}* cells, *mito^{AID}* PAN cells exhibited an increase in the percentage of cells with misoriented spindles in the presence of auxin (Figure 4(d)). These results indicate that even though PAN clusters form in buds that lack mitochondria, dynein function is still compromised in these cells. Thus, the role of mitochondria in regulating dynein function extends beyond simply concentrating Num1; mitochondria likely promote an arrangement of Num1 within a cluster that is competent for dynein anchoring.

Discussion

We developed a system to target and synthetically cluster Num1 on the plasma membrane and demonstrated that this system bypasses the requirement for mitochondria in Num1 cluster formation [17]. Thus, we were able to use this system to examine the role for mitochondria in dynein anchoring beyond concentrating Num1 in

clusters at the cell cortex. We found that mitochondria impact the ability of Num1 to anchor dynein even when mitochondria are no longer required for cluster formation (Figure 4(e)). The exact mechanistic contributions of mitochondria to dynein anchoring have yet to be determined, but several, non-mutually exclusive possibilities for how mitochondria may facilitate the ability of a cluster to anchor dynein can be envisioned. Mitochondria may promote an arrangement of Num1 within a cluster that is favorable for the interaction with dynein. For example, mitochondria may bring Num1 molecules into closer proximity thereby increasing the density of Num1 molecules within a cluster to facilitate dynein anchoring. The number of Num1 molecules in a wildtype cluster is estimated to be ~ 14 on average [14], while the number of dynein molecules within a cortically anchored dynein focus is estimated to be ~ 6 on average [27]. Thus, it is possible that several Num1 molecules may be required to anchor a dynein dimer. Alternatively, the interaction with mitochondria may drive a conformational change within Num1 itself that favors the interaction with dynein. This is an intriguing possibility as mitochondria and dynein both interact with the CC domain of Num1 [10–12]. In addition, Num1 is proposed to directly activate dynein [18,19,28]. Thus, the mitochondria-dependent arrangement of Num1 within a cluster may also impact the ability of Num1 to activate dynein. It is possible that mitochondria also create a unique microenvironment at the site of contact with the plasma membrane and cortical ER [29] that influences dynein anchoring and activation by mechanisms yet to be determined.

In cells in which Num1 is synthetically clustered, we observed an increase in the number of mitochondria-associated clusters per cell. This increase may be a result of increased levels of Num1 in PAN cells in comparison to wildtype cells. Alternatively, the clustering of Num1 may be a limiting step in the formation of a mitochondrial tether. We have proposed that the interaction of Num1 with mitochondria drives the assembly of Num1 clusters by inducing conformational changes within Num1 that are favorable for cluster assembly [17]. Cluster assembly, in turn, increases the avidity between Num1 and its binding partners

and, consequently, the ability of Num1 to robustly tether mitochondria. In a wildtype scenario, not all circumstances of proximity between mitochondria and the plasma membrane result in the formation of a Num1 cluster [17], suggesting that additional factors contribute to Num1 assembly and the formation of a productive mitochondrial tether. By synthetically clustering Num1, a likely initial limiting step in the formation of a mitochondrial tether, concentrating Num1, is bypassed. The increased local concentration of mitochondrial-binding sites within a synthetic Num1 cluster, in comparison to non-clustered Num1, likely stabilizes the interaction between the cluster and any part of the mitochondrial network that comes in contact with the cluster. In addition, the synthetic system creates stable clusters that decrease the dynamics of Num1 at the plasma membrane, which may also favor mitochondrial tethering. A similar scenario is observed for wildtype Num1 clusters, which once assembled are stationary, display limited exchange with the non-assembled pool, and persistently tether mitochondria for extended periods of time [5,17]. Interestingly, only a subset of PAN clusters tether mitochondria. This result raises the non-mutually exclusive possibilities that: 1) PAN clusters that serve as mitochondrial tethers are ones that mitochondria come in close proximity to by chance, or 2) additional factors, such as cortical ER, impact the ability of PAN clusters to anchor mitochondria [10].

Our examination of the role mitochondria play in dynein anchoring clearly demonstrates a role for mitochondria beyond simply clustering the anchor protein. Thus, mitochondria not only impact when and where the dynein anchor concentrates on the plasma membrane, but also have a yet to be determined role in dynein anchoring downstream of cluster formation. This adds yet another function to the mitochondria-PM contact sites that are generated and maintained by Num1, further highlighting that mitochondrial anchoring has functional consequences that extend beyond mitochondrial positioning to other critical cellular processes [30]. Going forward, it will be exciting to understand the full mechanistic contributions of mitochondria to dynein function, examine whether a role for mitochondria in dynein anchoring is conserved, and address the physiological significance of mitochondria-dependent dynein anchoring.

Materials and methods

Strains and plasmids

Strains W303 (*ade2-1; leu2-3; his3-11, 15; trp1-1; ura3-1; can1-100*) [31], W303 *NUM1-yEGFP::HIS*, W303 Δ *num1::HIS*, W303 Δ *dyn1::HIS*, and W303 *fzo1-1* Δ *dnm1::HIS* Δ *num1::KAN* [10], W303 *NUM1-yEGFP::KAN* [12], W303 *fzo1-1* [24], and W303 *DYN1-mKate::HIS*, Δ *kar9::NATNT2*, and W303 *MMR1-AID-FLAG::HYG* Δ *ypt11::NATNT2 TIR1::URA* (*mito^{AID}*) [17] were described previously.

The plasmids pXY142-mitodsRED (mitoRED) [32], p412-ADH1 *mitoTagBFP* (*mitoBFP::LEU*) [12], p416ADH1 *mitotagBFP* (*mitoBFP::URA*), *Ruby-Tub1::LEU*, and pFA6-link-mKate-*spHIS5* [17], pKT127 pFA6-link-yEGFP-KAN, pKT209 pFA6-link-yEGFP-CaURA3, and pKT128 pFA6a-link-yEGFP-SpHIS5 [33], p416-ADH1 and p414-MET25 [34] were described previously. pHIS3p: *mRuby2-Tub1 + 3'UTR::HPH* (*Ruby-Tub1::HYG*) (Addgene plasmids #50,633) was a gift from W. Lee, UMass Amherst [35]. *Ruby-Tub1::HYG* was digested with XbaI prior to transformation into yeast. pET21-pelB-LaG16 was a gift from J. Brickner, Northwestern University, and was originally obtained from M. Rout, The Rockefeller University [23]. LaG16 stands for llama antibody (nanobody) against GFP and will be referred to as α GFP. pFA6a-natMX6-PADH-3HA was purchased from Euroscarf (plasmid # P30346) [36]. pNHK53 (YIp, *ADH1::OsTIR1-9Myc1*) (*TIR1*) was obtained from the National BioResource Project, Japan (depositor: M. Kanemaki) [37].

pLL599 (pFA6-link-LaG16-CaURA3) was constructed by PCR amplifying LaG16 from pET21-pelB-LaG16 and inserting the product into pKT209 pFA6-link-yEGFP-CaURA3 using PacI and AscI sites.

pLL618 (pFA6-link-mKate-NATMX6) was constructed by PCR amplifying the NATMX6 cassette from pFA6a-natMX6-PADH-3HA and inserting the product into pFA6-link-mKate-*spHIS5* using BglII and EcoRI sites.

p414ADH1 *mitoTagBFP* (*mitoBFP::TRP*) was constructed by PCR amplifying *ADH1::mitoTagBFP* from p416ADH1 *mitoTagBFP* and inserting the product into SacI/XhoI digested p414-MET25 by gap repair.

W303 $\Delta dnm1::NATNT2$ was obtained by replacing the complete ORF of the gene with the indicated cassette using PCR-based targeted homologous recombination [38]. W303 $fzo1-1::KAN$ was a gift from J. Nunnari, University of California, Davis. W303 $NUM1\Delta CC\Delta PH-yEGFP::HIS$ was obtained by PCR-based targeted homologous recombination into W303 $\Delta num1$ cells. The functional C-terminally tagged W303 $NUM1\Delta PH-yEGFP::HIS$ ($NUM1\Delta PH$ encodes amino acids 1–2562 of Num1), W303 $PIL1-yEGFP::HIS$, and W303 $LSP1-mKate::NATMX6$ were constructed by PCR-based targeted homologous recombination using pKT128 pFA6a-link-yEGFP-SpHIS5 and pLL618 pFA6-link-mKate-NATMX6. W303 $PIL1-LaG16::CaURA$ ($PIL1-\alpha GFP$) was constructed by PCR-based targeted homologous recombination using pLL599 pFA6-link-LaG16-CaURA3. Haploid mutant/tagged strains were generated by crossing, followed by sporulation, and tetrad analysis.

Imaging

For Figures 1(c-d) and 2(a), W303 $NUM1-yEGFP$, W303 $NUM1\Delta PH-yEGFP$, W303 $PIL1-\alpha GFP$ $NUM1\Delta PH-yEGFP$, W303 $NUM1\Delta CC\Delta PH-yEGFP$, and W303 $PIL1-\alpha GFP$ $NUM1\Delta CC\Delta PH-yEGFP$ cells harboring mitoRED were grown to mid-log phase in synthetic complete (SC) – LEU + 2% (w/v) dextrose media with 2X adenine. W303 $PIL1-yEGFP$, W303 $NUM1-yEGFP$ $LSP1-mKate$, W303 $PIL1-yEGFP$ $LSP1-mKate$, and W303 $PIL1-\alpha GFP$ $NUM1\Delta PH-yEGFP$ $LSP1-mKate$ cells were grown to mid-log phase in SC + 2% (w/v) dextrose media with 2X adenine.

For Figure 3(b-d), W303 wildtype, W303 $\Delta dyn1$, W303 $\Delta num1$, W303 $NUM1\Delta PH$, $PIL1-\alpha GFP$ $NUM1\Delta PH-yEGFP$, W303 $\Delta kar9$, W303 $NUM1\Delta PH$ $\Delta kar9$, and W303 $PIL1-\alpha GFP$ $NUM1\Delta PH$ $\Delta kar9$ cells harboring Ruby-Tub1::HYG were grown to mid-log phase in SC + 2% (w/v) dextrose media with 2X adenine.

For Figure 4(a-b), W303 $NUM1-yEGFP$ $DYN1-mKate$ cells harboring mitoBFP::URA were grown to mid-log phase in SC-URA + 2% (w/v) dextrose media with 2X adenine. W303 $PIL1-\alpha GFP$ $NUM1\Delta PH-yEGFP$ $DYN1-mKate$ harboring mitoBFP::TRP were grown to mid-log phase in

SC-TRP + 2% (w/v) dextrose media with 2X adenine.

For Figure 4(c-d), W303 $mito^{AID}$ $NUM1-yEGFP$ and W303 $mito^{AID}$ $NUM1\Delta PH-yEGFP$ cells harboring Ruby-Tub1::LEU and mitoBFP::TRP were grown in SC-TRP + 2% (w/v) dextrose media with 2X adenine, pH = 6.4 media at 30°C for 2 hours. W303 $PIL1-\alpha GFP$ $mito^{AID}$ $NUM1\Delta PH-yEGFP$ cells harboring Ruby-Tub1::HYG and mitoBFP::LEU were grown in SC-LEU + 2% (w/v) dextrose media with 2X adenine, pH = 6.4 media at 30°C for 2 hours. DMSO or auxin (HiMedia, <http://www.himedialabs.com/TD/RM575.pdf>), to a final concentration of 1mM, was added and cells were grown for an additional 3 hours at 30°C.

For all imaging, cells were concentrated by centrifugation and mounted on a 4% w/v agarose pad. All imaging was performed at 24°C. Z-series of cells were imaged at a single time point or over time using a Leica Spinning Disk Confocal System (Leica) fit with a CSU-X1 spinning disk head (Yokogawa), a PLAN APO 100X, 1.44 NA objective (Leica), and an Evolve 512 Delta EMCCD camera (Photometrics). A step size of 0.4 μ m for Figures 1(d), 3(b) and 4(a and c) or 0.2 μ m for Figures 1(c) and 2(a) was used. Image capture was done using Metamorph (Molecular Devices). The images were deconvolved using AutoQuant X3's (Media Cybernetics) iterative, constrained three-dimensional deconvolution method. Single focal planes or maximum intensity projections, as indicated in the figure legends, are shown. To create maximum intensity projections, the maximum intensity Z-projection feature for stacks in FIJI was used. FIJI and Photoshop (Adobe) were used to make linear adjustments to brightness and contrast. Deconvolved images are shown. Pearson's correlation coefficients were determined using the colocalization feature in AutoQuant X3's (Media Cybernetics) on whole field views.

A cluster is defined as an accumulation of Num1 above the background signal that persists for at least 3 frames of imaging (> 1.5 min). The dimmer accumulations of Num1 that do not result in a productive cluster or tether point are dynamic and do not persist over multiple frames. For quantification of tether points, mitochondria had to remain associated with a Num1 cluster for \geq 1.5 minutes for the cluster to be considered a

tether. For quantification of cortical dynein foci, a Dyn1-mKate focus had to remain stable at the cell cortex for ≥ 1.5 minutes.

For the quantification of spindle orientation [17], large budded cells with spindles $> 1.25\mu\text{m}$ were analyzed [39]. To be correctly oriented, the spindle needed to cross the mother-bud neck or be within 45° of a line perpendicular to the neck. Misoriented spindles did not cross the neck and were more than 45° off of the mother-bud axis. Measurements of bud size, spindle length, and orientation were all done in FIJI.

Western blot

The indicated strains were grown to midlog phase in yeast extract, peptone + 2% (wt/vol) dextrose (YPD) media. 1.0 OD of cells were harvested, and whole cell extracts were prepared using a NaOH lysis and TCA precipitation procedure. Each TCA pellet was resuspended in 75 μl MURB (100 mM MES, pH 7, 1% SDS, and 3 M urea). Whole cell extracts were run on 3–8% Tris-Acetate gels (ThermoFisher, <https://www.thermofisher.com/order/catalog/product/EA03785BOX>) in denaturing conditions followed by western analysis using anti-GFP (ThermoFischer, <https://www.thermofisher.com/antibody/product/GFP-Tag-Antibody-Polyclonal/A-11122>) and anti-glucose-6-phosphate dehydrogenase (G-6-PDH; Sigma-Aldrich, <https://www.sigmaaldrich.com/catalog/product/sigma/a9521?lang=en®ion=US>) as the primary antibodies and goat anti-rabbit IgG DyLight 800 (ThermoFisher, <https://www.thermofisher.com/antibody/product/Goat-anti-Rabbit-IgG-H-L-Secondary-Antibody-Polyclonal/SA5-35571>), respectively, as the secondary antibodies. The immunoreactive bands were detected with the Odyssey Infrared Imaging System (LI-COR Biosciences).

Growth assays

For analysis of growth by serial dilution, cells were grown overnight in YPD (rich) media, pelleted, and resuspended in water at a concentration of 0.2 OD₆₀₀/ml, and tenfold serial dilutions were performed. Cells were spotted onto YPD plates and grown at 24°C, 30°C, or 37°C, as indicated.

Acknowledgments

We thank members of the Lackner lab, Jennifer Brace, members of the Weiss Lab, and the WiLa ICB for suggestions and critical scientific discussions. We thank Jason Brickner and Michael Rout for sharing the plasmid pET21-pelB-LaG16. We thank Jessica Hornick and instrumentation support from the Biological Imaging Facility at Northwestern University. L.M.K. is supported by the NIH NIGMS Training Grant T32GM008061. L.L.L. is supported by the NIH NIGMS grant R01GM120303 and the Robert H. Lurie Comprehensive Cancer Center – The Lefkofsky Family Foundation/Liz and Eric Lefkofsky Innovation Research Award. In addition, this work was funded in part by the Chicago Biomedical Consortium with support from the Searle Funds at The Chicago Community Trust.

Disclosure statement

No potential conflict of interest was reported by the authors.

Funding

This work was supported by the National Institute of General Medical Sciences [R01GM120303, T32GM008061]; Chicago Biomedical Consortium [C-073].

ORCID

Laura L. Lackner  <http://orcid.org/0000-0003-0311-5199>

References

- [1] Kormanec J, Schaaff-Gerstenschlager I, Zimmermann FK, et al. Nuclear migration in *Saccharomyces cerevisiae* is controlled by the highly repetitive 313 kDa NUM1 protein. *Mol Gen Genet.* 1991;230:277–287. PMID:1745235.
- [2] Eshel D, Urrestarazu LA, Vissers S, et al. Cytoplasmic dynein is required for normal nuclear segregation in yeast. *Proc Natl Acad Sci U S A.* 1993;90:11172–11176. PMID:8248224
- [3] Li YY, Yeh E, Hays T, et al. Disruption of mitotic spindle orientation in a yeast dynein mutant. *Proc Natl Acad Sci U S A.* 1993;90:10096–10100. PMID:8234262
- [4] Adames NR, Cooper JA. Microtubule interactions with the cell cortex causing nuclear movements in *Saccharomyces cerevisiae*. *J Cell Biol.* 2000;149:863–874. PMID:10811827.
- [5] Heil-Chapdelaine RA, Oberle JR, Cooper JA. The cortical protein Num1p is essential for dynein-dependent interactions of microtubules with the cortex. *J Cell Biol.* 2000;151:1337–1344. PMID:11121446.

- [6] Farkasovsky M, Kuntzel H. Cortical Num1p interacts with the dynein intermediate chain Pac11p and cytoplasmic microtubules in budding yeast. *J Cell Biol.* **2001**;152:251–262. PMID:11266443.
- [7] Markus SM, Lee WL. Regulated offloading of cytoplasmic dynein from microtubule plus ends to the cortex. *Dev Cell.* **2011**;20:639–651. PMID:21571221.
- [8] Cerveny KL, Studer SL, Jensen RE, et al. Yeast mitochondrial division and distribution require the cortical Num1 protein. *Dev Cell.* **2007**;12:363–375. PMID:17336903.
- [9] Klecker T, Scholz D, Fortsch J, et al. The yeast cell cortical protein Num1 integrates mitochondrial dynamics into cellular architecture. *J Cell Sci.* **2013**;126:2924–2930. PMID:23641071.
- [10] Lackner LL, Ping H, Graef M, et al. Endoplasmic reticulum-associated mitochondria-cortex tether functions in the distribution and inheritance of mitochondria. *Proc Natl Acad Sci U S A.* **2013**;110:E458–E467. PMID:23341591.
- [11] Tang X, Germain BS, Lee WL. A novel patch assembly domain in Num1 mediates dynein anchoring at the cortex during spindle positioning. *J Cell Biol.* **2012**;196:743–756. PMID:22431751.
- [12] Ping HA, Kraft LM, Chen W, et al. Num1 anchors mitochondria to the plasma membrane via two domains with different lipid binding specificities. *J Cell Biol.* **2016**;213:513–524. PMID:27241910.
- [13] Yu JW, Mendrola JM, Audhya A, et al. Genome-wide analysis of membrane targeting by *S. cerevisiae* pleckstrin homology domains. *Mol Cell.* **2004**;13:677–688. PMID:15023338.
- [14] Tang X, Punch JJ, Lee WL. A CAAX motif can compensate for the PH domain of Num1 for cortical dynein attachment. *Cell Cycle.* **2009**;8:3182–3190. PMID:19755860.
- [15] Farkasovsky M, Kuntzel H. Yeast Num1p associates with the mother cell cortex during S/G2 phase and affects microtubular functions. *J Cell Biol.* **1995**;131:1003–1014. PMID:7490278.
- [16] Chao JT, Wong AK, Tavassoli S, et al. Polarization of the endoplasmic reticulum by ER-septin tethering. *Cell.* **2014**;158:620–632. PMID:25083872.
- [17] Kraft LM, Lackner LL. Mitochondria-driven assembly of a cortical anchor for mitochondria and dynein. *J Cell Biol.* **2017**;216:3061–3071. PMID:28835466.
- [18] Lammers LG, Markus SM. The dynein cortical anchor Num1 activates dynein motility by relieving Pac1/LIS1-mediated inhibition. *J Cell Biol.* **2015**;211:309–322. PMID:26483554.
- [19] Ananthanarayanan V. Activation of the motor protein upon attachment: anchors weigh in on cytoplasmic dynein regulation. *Bioessays.* **2016**;38:514–525. PMID:27143631.
- [20] Walther TC, Brickner JH, Aguilar PS, et al. Eisosomes mark static sites of endocytosis. *Nature.* **2006**;439:998–1003. PMID:16496001.
- [21] Olivera-Couto A, Aguilar PS. Eisosomes and plasma membrane organization. *Mol Genet Genomics.* **2012**;287:607–620. PMID:22797686.
- [22] Muyldermans S. Nanobodies: natural single-domain antibodies. *Annu Rev Biochem.* **2013**;82:775–797. PMID:23495938.
- [23] Fridy PC, Li Y, Keegan S, et al. A robust pipeline for rapid production of versatile nanobody repertoires. *Nat Methods.* **2014**;11:1253–1260. PMID:25362362.
- [24] Hermann GJ, Thatcher JW, Mills JP, et al. Mitochondrial fusion in yeast requires the transmembrane GTPase Fzo1p. *J Cell Biol.* **1998**;143:359–373. PMID:9786948.
- [25] Miller RK, Rose MD. Kar9p is a novel cortical protein required for cytoplasmic microtubule orientation in yeast. *J Cell Biol.* **1998**;140:377–390. PMID:9442113.
- [26] Yin H, Pruyne D, Huffaker TC, et al. Myosin V orientates the mitotic spindle in yeast. *Nature.* **2000**;406:1013–1015. PMID:10984058.
- [27] Markus SM, Plevock KM, St Germain BJ, et al. Quantitative analysis of Pac1/LIS1-mediated dynein targeting: implications for regulation of dynein activity in budding yeast. *Cytoskeleton (Hoboken).* **2011**;68:157–174. PMID:21294277.
- [28] Ananthanarayanan V, Schattat M, Vogel SK, et al. Dynein motion switches from diffusive to directed upon cortical anchoring. *Cell.* **2013**;153:1526–1536. PMID:23791180.
- [29] Prinz WA. Bridging the gap: membrane contact sites in signaling, metabolism, and organelle dynamics. *J Cell Biol.* **2014**;205:759–769. PMID:24958771.
- [30] Kraft LM, Lackner LL. Mitochondrial anchors: positioning mitochondria and more. *Biochem Biophys Res Commun.* **2018**;500:2–8. PMID:28676393.
- [31] Naylor K, Ingerman E, Okreglak V, et al. Mdv1 interacts with assembled Dnm1 to promote mitochondrial division. *J Biol Chem.* **2006**;281:2177–2183. PMID:16272155.
- [32] Friedman JR, Lackner LL, West M, et al. ER tubules mark sites of mitochondrial division. *Science.* **2011**;334:358–362. PMID:21885730.
- [33] Sheff MA, Thorn KS. Optimized cassettes for fluorescent protein tagging in *Saccharomyces cerevisiae*. *Yeast.* **2004**;21:661–670. PMID:15197731.
- [34] Mumberg D, Muller R, Funk M. Yeast vectors for the controlled expression of heterologous proteins in different genetic backgrounds. *Gene.* **1995**;156:119–122. PMID:7737504.
- [35] Markus SM, Omer S, Baranowski K, et al. Improved plasmids for fluorescent protein tagging of microtubules in *saccharomyces cerevisiae*. *Traffic.* **2015**;16:773–786. PMID:25711127.
- [36] Van Driessche B, Tafforeau L, Hentges P, et al. Additional vectors for PCR-based gene tagging in *Saccharomyces cerevisiae* and *Schizosaccharomyces pombe* using nourseothricin resistance. *Yeast.* **2005**;22:1061–1068. PMID:16200506.

- [37] Nishimura K, Fukagawa T, Takisawa H, et al. An auxin-based degron system for the rapid depletion of proteins in nonplant cells. *Nat Methods*. 2009;6:917–922. PMID:19915560.
- [38] Janke C, Magiera MM, Rathfelder N, et al. A versatile toolbox for PCR-based tagging of yeast genes: new fluorescent proteins, more markers and promoter substitution cassettes. *Yeast*. 2004;21:947–962. PMID:15334558.
- [39] Moore JK, Li J, Cooper JA. Dynactin function in mitotic spindle positioning. *Traffic*. 2008;9:510–527. PMID:18221362.